



Automated SEM study of PGM distribution across a UG2 flotation concentrate bank: implications for understanding PGM floatability

by D. Chetty*, L. Gryffenberg*, T.B. Lekgetho†, and I.J. Molebale‡

Synopsis

The characterization of platinum group minerals (PGMs) from concentrator circuits provides valuable information towards understanding PGM recovery under given milling and flotation conditions. Additional mineralogical characterization also provides information on ore variability, which may affect recovery. Considering the low grades involved, automated scanning electron microscopy (SEM) characterization of PGMs has enabled relatively quick analyses, compared with older, time consuming and less accurate optical microscopy methods. Over the years, parameters, such as species, size distribution, liberation, gangue and base metal sulfide (BMS) associations, have been used to characterize the PGMs in a process mineralogical context, to aid metallurgical interpretation.

This paper considers whether flotation indices determined for PGMs can be empirically validated, using initial results from analysis of PGMs in a concentrate bank from a South African concentrator treating UG2 ore from the western limb of the Bushveld Complex. The aim is to determine whether floatability is adequately described by these parameters, or whether other mineralogical factors must be considered when assessing PGM floatability, and hence accounting for recovery vs. losses to tails.

The data obtained to date, show that flotation parameters (including liberation index, BMS/gangue relationships and size distribution) have merits where large changes in PGM concentration occur, as observed in the first four cells of the concentrate bank. Larger data sets, however, are required to assess floatability, particularly where concentrate cell grades are similar, as observed in the last six cells of the concentrate bank. Furthermore, the floatability indices could be enhanced by the incorporation of selected associated gangue mineral information, chief amongst these being the content and mode of occurrence of naturally floatable talc and associated orthopyroxene.

in metallurgical test work undertaken at Mintek. Over the years, a characterization scheme for PGM in flotation feeds, concentrates and tails, has been devised to assist in assessing metallurgical performance. This was largely based on the early efforts of Penberthy (2001), who investigated the geometallurgical characteristics of UG2 ore by studying geological effects on the chromitite and relating these to PGM flotation characteristics from batch flotation tests. The premise of the classification scheme is that PGM floatability is related to the parameters of species, grain size and mode of occurrence.

The type of PGM species is largely only relevant to floatability if liberated PGMs are considered, in which case species can be directly correlated with flotation response. PGM floatability, in terms of species, has more recently been given attention, in ores such as the Platreef and Great Dyke, where PGE-tellurides and arsenides are more abundant compared with sulfides (Shackleton *et al.*, 2007a, b; Shamaila and O'Connor, 2008; Vermaak *et al.*, 2007). The grain size of PGMs has also been considered to affect floatability, with very fine (i.e. $<3 \mu\text{m}$) PGMs considered as slow floaters (Penberthy *et al.*, 2000).

The mode of occurrence of PGMs encompasses the degree of PGM liberation, and association with base metal sulfide (BMS) and gangue minerals. Liberation is not a straightforward description as might be found, for example, with BMS flotation or leach process mineralogical investigations. Because flotation of PGMs is based on bulk sulfide flotation principles (Xiao and Laplante, 2004; O'Connor,

Introduction

Platinum group minerals (PGMs) are those minerals containing any of the platinum group elements (PGE): Pt, Pd, Rh, Ru, Ir and Os. In UG2 ore of the Bushveld Complex, these typically occur as sulfides, alloys, and to a lesser extent, as arsenides and tellurides, with fine grain sizes, generally $<10 \mu\text{m}$ (McLaren and de Villiers, 1982; Penberthy *et al.*, 2000). Their characterization is an integral component

* Mineralogy Division, Mintek, Randburg, South Africa.

† Department of Geology, University of the Free State.

‡ Department of Geology, University of Pretoria.

© The Southern African Institute of Mining and Metallurgy, 2009. SA ISSN 0038-223X/3.00 + 0.00. Paper received Jul. 2009; revised paper received Sep. 2009.

Automated SEM study of PGM distribution across a UG2 flotation concentrate

2005), the association of PGM with BMS is as important as, if not more important than, liberated PGM for floatability (e.g. Penberthy, 2001). In the same vein, PGM association with gangue minerals may or may not contribute to increased floatability, as this is more likely a function of gangue floatability, which presents its own set of challenges for concentrate grades and element specifications through dilution and entrainment effects.

In order to assess how effectively PGM characterization parameters describe floatability, a UG2 flotation concentrate bank was sampled from the primary circuit of a South African MF2 (mill-float-mill-float) concentrator treating ore from the western limb of the Bushveld Complex. The concentrates were subjected to analysis using automated scanning electron microscopy (SEM), allowing for at least 250 PGM grains to be assessed per concentrate. Since a concentrate bank allows more 'opportunity' for PGM flotation from the first to the last flotation cell, floatability is expected to decrease from the first to the last cell in the bank, before non-floatable PGMs report to the tails. Further, since ~70 % of the PGMs are recovered in the primary rougher circuit, sampling of the concentrate bank would be expected to provide the best opportunity for finding PGM grains.

Methods

For the primary circuit sampled, UG2 ore milled to 40% < 75 μm was fed into the flotation cells with 10 forced air tank cells (20 m³) constituting the concentrate bank. The reagents used for flotation were copper sulfate (activator), sodium isobutyl xanthate (collector), carboxy-methyl-cellulose (CMC) (depressant) and methyl isobutyl carbinol (MIBC) (frother). After the cascading flotation through the 10 primary cells, the tails were discharged to the secondary ball mill, before entry to the secondary, rougher circuit. The primary rougher feed (PRF), ten primary rougher concentrates (PRC1 to 10) and primary rougher tail (PRT) were sampled over a four hour period, during which plant stability was maintained (Figure 1).

After weighing, drying and blending of the slurries, representative sub-samples were taken for PGE analysis by fire assay and inductively-coupled plasma-optical emission spectroscopy (ICP-OES), and polished section preparation for automated SEM studies. The polished sections were analysed using a Mineral Liberation Analyser (MLA), employing the automated sparse phase search with dual zoom (SPL_DZ) method (Fandrich *et al.*, 2007). Owing to the extremely small

size of PGM grains, most often <10 μm in section, the method involves the scanning of the section at a given magnification, to find 'bright' phases above a specified backscatter electron intensity (to which PGMs are amenable), upon which such phases, together with associated phases in a particle, are distinguished by X-ray spectral analysis and mapped at high resolution. Note that phases are seen in two dimensions as grains, by virtue of their backscattered electron intensity. Two or more grains that share their edges make up a particle; a single grain, where liberated, will also be a particle. Data outputs take the form of false-colour particle maps of the bright phase, which have been generated through processing against a standards file. The standards file comprises energy dispersive spectra (EDS) collected from the various phases present (e.g. PtS, orthopyroxene), against which the collected X-ray spectra of the automated analysis are compared and identified by the best match principle, with some manual intervention necessary to ensure that maps are representative of the grains identified. The quantitative phase data are then reduced further, offline.

As with any analytical technique, data quality must be accounted for, particularly where data comparisons are made. Although automated SEM techniques are relatively rapid at finding minerals with grades in the ppm range, large amounts of data are still necessary to ensure accuracy. Considering that large tonnages of ore are routinely processed at PGM concentrators, and that substantially less than 1 g of material is actually analysed to look for PGMs in a dozen polished sections, representative sub sampling is imperative. Further, owing to the high variability in PGM characteristics, the number of such grains analysed needs to be substantial, a problem not easily overcome, in spite of automation. Studies making use of automated SEM data provide worryingly inadequate information on this aspect. Accordingly, it is worth stating that data collection is a continuous process in this study. This paper presents data for a total of 4513 PGM grains obtained to date across a primary rougher circuit, 4199 of which are derived from concentrates (Table I). Attempts have been made to place uncertainties on the data, since these are necessary when comparing the PGM distribution as the flotation proceeds down the bank of cells. The uncertainties were obtained by using a form of resampling statistics, with replacement. This involved simulation of a parameter by resampling different aliquots from the same bulk population a thousand times, to arrive at a mean value for the parameter, as well as its associated

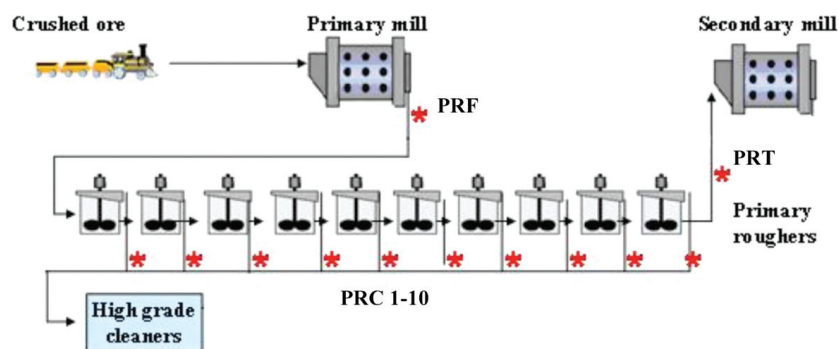


Figure 1—Overview of the primary rougher circuit, and sampled points(asterisks)

Automated SEM study of PGM distribution across a UG2 flotation concentrate

Table I

Number of PGM grains encountered in polished sections analysed to date

Sample	Number of grains	Number of liberated PGM grains
PRF	198	70
PRC1	784	388
PRC2	465	235
PRC3	338	169
PRC4	456	204
PRC5	360	172
PRC6	414	160
PRC7	321	130
PRC8	288	115
PRC9	410	147
PRC10	363	148
PRT	116	9
TOTAL	4513	1947

uncertainty (Wikipedia, accessed May 2009). Simulations were performed using the @Risk software (Palisade Corporation), which uses Monte Carlo simulation on the Excel platform.

Results and discussion

PGE assays

Concentrations for Pt, Pd, Rh, Ru and Ir are presented in Figure 2. The concentration for each of the PGEs decreases in a steady fashion from PRC1 to PRC10, with PRT containing the lowest concentrations. Additionally, PRC1 and PRC2 concentrate the bulk of the PGEs in the bank, and account for ~60 % recovery, with the subsequent concentrate cells only accounting for another ~10 % recovery before PGEs report to the tails. The Pt:Pd ratio is smaller in PRC1 than in PRC2 and cells further down the bank, indicating a stronger concentration of Pd in PRC1 relative to PRC2, when compared with Pt. The same appears to hold for Ru as the third most abundant PGE in the bank.

Automated SEM data quality

Following the example of Penberthy (2001), the resampling technique was applied here to the PRC1 sample, using data on 784 grains of PGM. The uncertainty was calculated on the grouped modal data for a random sample aliquot of 200 grains (Table II), at the 90 % confidence limit. The exercise was repeated for the grain size parameter (Table III).

The uncertainties obtained (Tables II and III) confirm the need for large amounts of data required for meaningful information on aspects such as modal proportions of lesser PGM species and size classes >15 μm . Therefore, the more detailed the information sought, the more data are required to provide such information (Merkle, 2005).

Providing a large dataset comes at the cost of instrument time, along with associated mineralogist time and consumables. Notwithstanding the advent of new field emission gun SEM systems that significantly reduce analytical time (Dobbe *et al.*, 2008), slower tungsten filament SEM systems are more dominantly in use worldwide (as in this study). Hypothetically, to analyse 500 PGM grains in

each of the feed and tails samples, as well as 1000 grains in each of ten concentrate samples, a timeframe of ~6 months in instrument and associated mineralogist time is calculated (for a single tungsten filament system). Added to this, is another 3 months of offline data processing, reporting and interpretation, at a minimum instrument efficiency of 80 %.

Considering that the auto-SEM software does not cater for specific reporting (which comes at extra cost from suppliers), this timeframe takes into consideration data processing tools that must be custom-driven to handle large data sets and provide answers sought for the present study. Clearly, the

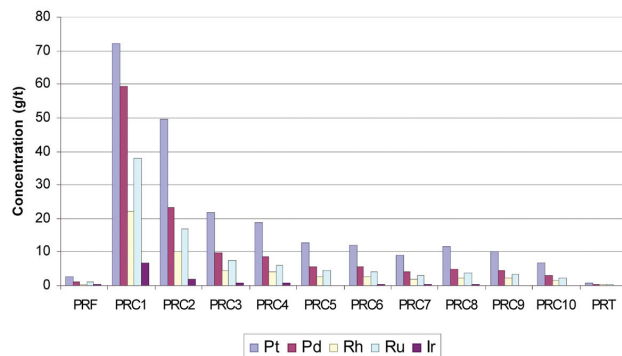


Figure 2—PGE distribution in the UG2 primary rougher circuit

Table II

Modal proportions of PGM groupings in PRC 1 and uncertainty (absolute) at the 90% confidence limit, associated with a sample aliquot of 200 grains, as calculated using resampling statistics.

PGM grouping	Modal abundance (%)	Uncertainty ($\pm\%$)
PGE Sulfides	93.65	3.34
PGE Alloys	4.24	3.13
PGE Arsenides	1.13	1.06
PGE Tellurides	0.75	0.84
PGE Bismuthotellurides	0.23	0.17

Table III

Size distribution class proportions in PRC 1 and uncertainty (absolute) at the 90% confidence limit, associated with a sample aliquot of 200 grains, as calculated using resampling statistics

Size class (ECD)	Relative abundance (vol%)	Uncertainty ($\pm\%$)
0-3	5.75	1.08
3-6	30.76	4.96
6-9	25.83	4.96
9-12	14.24	4.74
12-15	6.29	3.67
15-18	4.84	4.05
18-21	4.87	4.87
21-24	2.33	4.15
24-27	0.00	-
27-30	0.00	-
>30	5.10	8.61

Automated SEM study of PGM distribution across a UG2 flotation concentrate

time required is not trivial, and this possibly explains the lack of data quality criteria in published studies, for which minimal targets are dictated by instrument time and production constraints.

PGM species and their relative abundance

Twenty-three PGM species were classified from X-ray spectra of encountered PGM grains. Platinum group minerals are not assigned mineral names (since the technique is not suitable for quantitative mineral chemical analysis), but are rather named according to the elements for which peaks are encountered in the X-ray spectra, i.e. the chemical make-up of the grains. Grains, therefore, may be classified as sulfides, alloys, tellurides, bismuthotellurides, arsenides and other non-sulfides that include combinations of PGE, Sb, As and Sn (Table IV). A further advantage of this system of nomenclature is that it is metallurgically more meaningful than mineral names (e.g. PtS vs. cooperite).

Of the population of PGM grains analysed in each sample, PGE-sulfides dominate the assemblage, also evident in UG2 ore studied by Penberthy *et al.* (2000), constituting >90 vol% of the PGMs encountered. For the feed, ~93 vol% is PGE-sulfide, ~3 vol% is alloy, followed by ~2.5 vol% telluride, ~1 vol% as bismuthotelluride and <1 vol% as arsenide and others. Amongst the sulfides, four individual species are consistently present in the concentrates in amounts >10 vol% each: PtS, PtPdNiS, RuS and PtRhCuS. Interestingly, the ratio of Pt-bearing, non-Pd-bearing PGMs to Pd-bearing PGMs is smaller in PRC1 compared with PRC2, thus supporting the Pt:Pd ratios observed from the bulk PGE assays.

As indicated for floatability considerations, relative abundance of the different PGM species/groupings in each of the concentrate cells should be best considered only for liberated PGMs. This is addressed later in the paper.

PGM size distribution

It is worth noting that size analysis of PGMs in two dimensions results in an underestimation of true size, owing to stereological effects (e.g. Sutherland, 2007). Nevertheless, comparisons of size distribution should still be possible, given that all data were obtained in the same manner, and that sufficient numbers of grains are analysed. Size is reported in terms of an equivalent circle diameter (ECD), which is the diameter of a circle of area equivalent to that of the grain, and is given by $ECD = 2 \cdot \sqrt{\text{area}/\pi}$. Another important effect of size distribution is that of the nugget effect. Where unusually large grains are present, size can bias the contribution, in volume%, of such grains. In this instance, number% will be much less than volume%. On the other hand, numerous small grains would be required if they are to, collectively, contribute to the total volume. In such cases, number% is typically much larger than volume% contributions. The effects of nuggets are substantial if sufficient numbers of grains are not analysed to 'smooth out' the effect. For this reason, very large, single, grains contributing >5 to 10 vol% of the PGM population were omitted from the data set. As more data are generated, they will be reinstated, but at present, owing to the bias placed on the data, they are removed.

Notwithstanding the uncertainties associated with the various parameters, grain sizes for the PGM population as a

whole, suggest a broad trend of increasing contribution of the 0-3 μm size class to the overall PGM population down the concentrate bank, but more data would be required to verify this. Although smaller grain size might have an effect on floatability, this must be considered in the context of liberation characteristics, as 0-3 μm class grains are likely to be locked in, or attached to, gangue after a primary grind. The majority of grains, by volume, in all samples, reports to the >9 μm fraction (>60 vol%; Figure 3), with the cells from PRC8 generally slightly higher in concentration of the fraction, to PRC10, comprising >80 vol% of the fraction. No grains >15 μm in size were encountered in the tails.

PGM mode of occurrence

PGM mode of occurrence is considered for the PGM population as a whole, i.e. no species are differentiated. The mode of occurrence takes into account BMS and gangue (i.e.

Table IV

PGM species and groups identified from encountered grains

PGM groups	Individual species
PGE-sulfides	PtS PdS PtPdNiS PtRhS RuS PtRhCuS PtPdRhCuS PtPdAsS PtRhAsS
PGE-alloys	PtFe PdHg PdPb
PGE-arsenides	PdAs PtAs PtRuAs
PGE-bismuthotellurides	PtBiTe PdBiTe PtPdBiTe
PGE-tellurides	PtTe PtPdTe
PGE-Others	PdAsSb PdAsSn PtPdAsSn

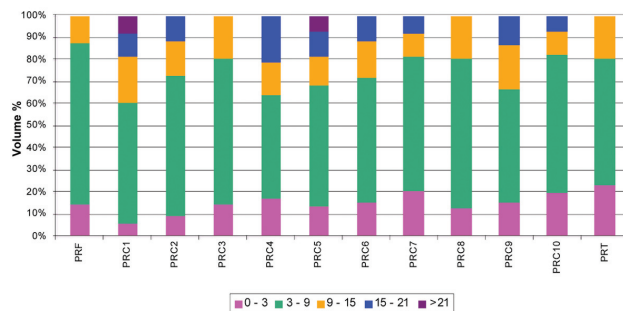
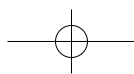


Figure 3—Size distribution, by volume, of PGM grains in the feed, tails and concentrates of the primary rougher circuit. Note that size classes are expressed in terms of ECD



Automated SEM study of PGM distribution across a UG2 flotation concentrate

silicate and chromite) associations, and a liberation index, similar to 'liberation by composition' (Petruk, 2000) is calculated. Mode of occurrence data are then combined with BMS and PGM grain sizes to obtain a floatability index, based on key size limitations identified for PGMs and BMS in floatability. In terms of liberation characteristics, the PGM and BMS are considered as valuable minerals for a classification scheme that involves the association between PGM, BMS and gangue (Table V).

For the primary rougher concentrates, the relative proportions, by volume, of the L particles decrease in a broad sense from PRC1 (~70 vol%) to PRC10 (~55 vol%) (Figure 4). For the combined L and SL classes, PRC1 and PRC2 display the highest proportions (~80 to 90 vol%), followed by PRC3 (~70 vol%), with all other cells containing below 60 vol% of the combined classes.

The rather erratic distribution of G classes might be attributed not only to the low amounts in the concentrates, but also to the nature of the gangue associated with the PGM. In the latter instance, it may well be the gangue that has caused the PGM to float, rather than the PGM pulling the gangue with it. The same reasoning would hold for the presence of the other composite particles in all the cells, particularly in the first few cells. The highest proportion of G, as expected, occurs in the tails sample. It would appear that the SAG class is significant in all the concentrates, and the presence of such particles in the concentrates suggests a complex interplay between relative gangue, BMS and PGM floatability characteristics in reporting these particles to the froth phase. As mentioned for gangue, the type of BMS associated with the PGM is of importance, since different BMS are known to display different floatability (e.g. Penberthy *et al.*, 2000; Becker *et al.*, 2008).

For the liberation index (LI), the combined PGM and BMS area is taken as a proportion of the total particle area. Hence, an index of 0.8-1 indicates a virtually liberated PGM and/or PGM-BMS particle, whereas an index <0.2 indicates that the PGM or PGM-BMS component is very low in proportion in the particle. It is generally expected that the higher the liberation index, the more floatable the particle will be, but the calculation does not take into account the key component of exposed surface of the PGM and BMS, and should therefore be used in conjunction with the liberation characteristics for assessing floatability.

As might be expected, the proportion of the 0.8-1 LI class is highest in PRC1, followed by PRC2 and PRC3. The volume distribution of particles of this class is then somewhat erratic

down the bank, before displaying its lowest abundance in the tails (Figure 5). The lowest LI class (<0.2) shows the opposite effect down the bank, before reaching its highest concentration in the tails. As with the liberation data, a complex pattern emerges in the PRC4-10 cells, owed to composite particles displaying the 0.2-0.8 LI characteristics.

In classifying PGM-containing particles, the mode of occurrence of the PGM grain has considered gangue and BMS associations, as well as proportions of PGM and BMS in particles. A further consideration must be the size of the PGM and BMS in conjunction with the gangue/BMS association. For this, a floatability index has been derived, which makes use of a PGM grain size of 3 µm and a BMS grain size of 10 µm (Table VI) in assessing floatability, based, in part, on the work of Penberthy (2001).

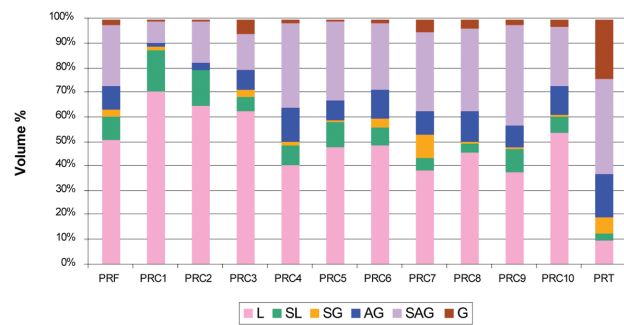


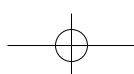
Figure 4—Liberation characteristics across the primary rougher circuit



Figure 5—Liberation index distribution across the primary rougher circuit

Class	Description
L	Liberated PGMs
SL	PGMs associated with liberated BMS
SG	PGMs associated with BMS locked in Silicate or Oxide gangue particles
AG	PGMs attached to Silicate or Oxide gangue particles
SAG	PGMs associated with BMS attached to Silicate or Oxide gangue particles
G	PGMs locked within Silicate or Oxide gangue particles

Fast Floating	Liberated PGMs >3µm ECD Liberated BMS >10µm ECD
Slow Floating 1	Liberated PGMs <3µm ECD Liberated BMS <10µm ECD PGMs > 3 µm ECD attached to gangue BMS >10 µm ECD attached to gangue
Slow Floating 2	PGMs < 3 µm ECD attached to gangue BMS <10 µm ECD attached to gangue
Non-floating	PGMs and/or BMS locked in gangue



Automated SEM study of PGM distribution across a UG2 flotation concentrate

Using the criteria for floatability index, a trend of decreasing abundance in fast-floating particles is observed from PRC1 to PRC4 (Figure 6), with erratic distribution to PRC10. Fast-floating particles are dominated by liberated PGMs >3 µm ECD, as opposed to BMS-PGM particles (Figure 7). Similarly, slow-floating 1 particles increase in abundance down the bank, albeit erratically, from PRC4 to PRC10. Slow floating 1 particles are dominated by PGMs associated with BMS >10 µm ECD attached to gangue (Figure 8), particularly from PRC4 to PRC10. The slow-floating 2 particles are erratically distributed across the bank, and are dominated by particles in which PGMs are associated with BMS <10 µm ECD attached to gangue; such particles are most abundant in PRC7 and PRC8 (Figure 9). The distributions in Figures 7, 8 and 9 will also be influenced by the type of BMS with which the PGMs are associated. Non floating particles, defined as PGMs and/or BMS locked in gangue, are erratically distributed (Figure 7). The combined slow and non floating categories are most abundant in the PRT. The unexpected high percentage of combined fast-floating and slow-floating 1 particles in the PRT requires further investigation.

PGM-BMS-Gangue composite particles

The SAG liberation class (Table V) represents the major composite PGM-bearing particle class across the concentrate bank (Figure 4). In all cases, pentlandite is the major BMS species in the SAG class, as indeed it is in the SL class, and the gangue minerals in SAG particles are predominantly orthopyroxene/talc, amphibole, chlorite and plagioclase. Minerals such as talc, talc altered orthopyroxene and chlorite are considered to be naturally floatable gangue (e.g. Becker

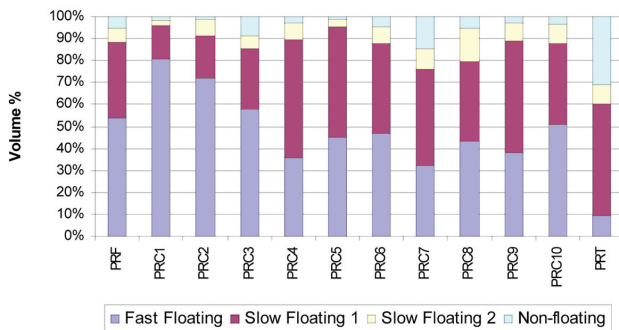


Figure 6—Floatability index across the primary rougher circuit

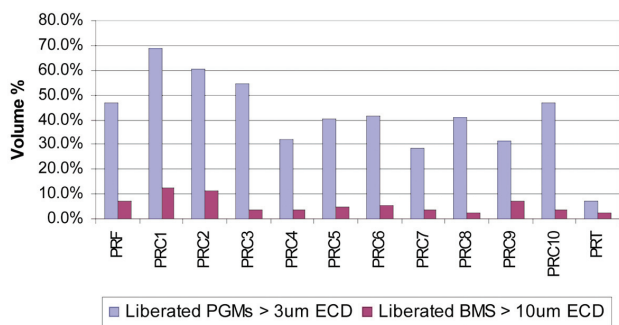


Figure 7—Distribution of fast-floating PGM-bearing particles across the primary rougher circuit

et al., 2008), and the presence of SAG and other gangue-composite PGM bearing particles in, particularly, the first few cells of the concentrate bank, may be, in part, due to naturally floatable gangue. Associations with plagioclase, on the other hand, may arise from the PGM/BMS component of the particle reporting it to the froth phase, although entrainment effects could also play a role.

Liberated PGM population

To assess the floatability of PGMs as a function of the species, the liberated PGMs must be considered, as well as their size distribution. Although the data will carry higher uncertainties owing to the smaller population dealt with (1947 grains; Table I), a few general comments can be made. The PGM sulfides dominate the population, but appear to decrease in abundance down the bank, with a peculiar drop in concentration in PRC7 that appears to be supported by the lower grade of PRC7 relative to its neighbouring cells (Figures 2 and 10).

The distribution of PGE alloys, arsenides and bismuthotellurides is difficult to adequately assess in the light of the poor statistics of liberated particles. Overall, these species tend to peak in concentration further down the bank, which suggests consistency with observations by Penberthy et al. (2000), but contrary to observations by Nel et al. (2005) who saw no hierarchy in floatability as a function of PGM species. The latter reference might be due to a smaller data set obtained on a feed sample, although no mention is made of the number of grains that were analysed.

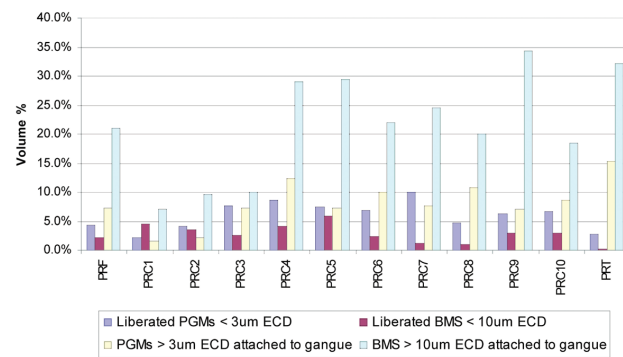


Figure 8—Distribution of Slow-floating 1 PGM-bearing particles across the primary rougher circuit

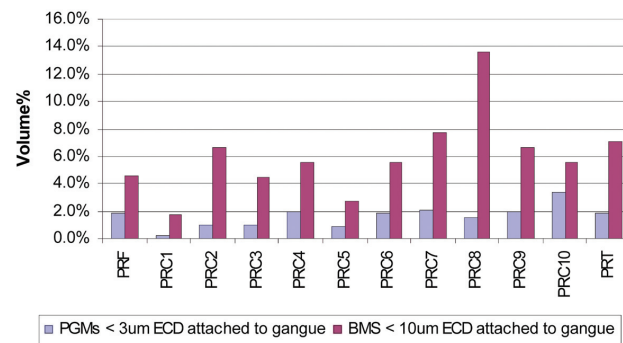


Figure 9—Distribution of Slow-floating 2 PGM-bearing particles across the primary rougher circuit

Automated SEM study of PGM distribution across a UG2 flotation concentrate

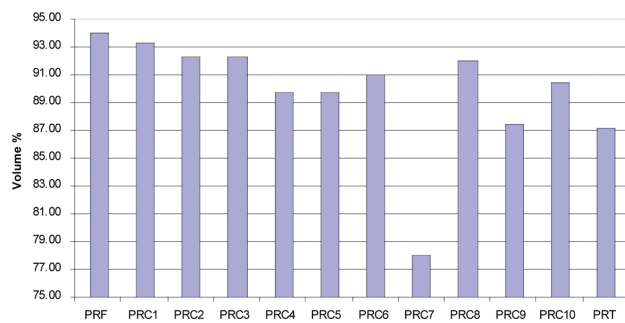


Figure 10—Relative abundance of PGE sulfides from the liberated PGM particle data set

Within species, no definitive decrease in particle size is noted down the concentrate bank, except perhaps with the sulfides, which display average ECDs of 4 to 5 μm in PRC1 and PRC2, before decreasing to <4 μm in average ECD for the other cells in the bank. This trend appears to correlate with the observation by Penberthy *et al.* (2000) that larger liberated PGM particles report to the faster-floating concentrates, based on batch flotation test work. For the other species, PGM particle size is erratic, and average ECDs of 6 μm are sometimes reached lower down the concentrate bank. The poor statistics associated with only a few grains render comparison meaningless, and the size distribution of liberated PGM species outside of the PGE-sulfides cannot be considered further for the present.

Conclusions

PGM characteristics, as determined from automated SEM analysis, have been put forth in this paper, based on 4199 PGM grains analysed across a UG2 primary rougher concentrate bank. Parameters include the PGM species and their relative abundance, PGM grain size distribution, and mode of occurrence. It is concluded that the floatability index, liberation index and liberation characteristics describe, relatively well, the behaviour of PGMs in the first three to four concentrate cells of the bank. However, behaviour in subsequent cells is not well explained by these parameters. This is largely a consequence of complex interplay amongst floatable and non floatable gangue, PGM and BMS, together with their respective grain size distributions. Whereas naturally floatable gangue minerals are routinely considered in metallurgical assessment of PGM behaviour in flotation, they are not quantitatively incorporated in aspects such as liberation index and floatability index. Such indices have relied on PGM and BMS as being the floatable components in particles, but should ideally include naturally floatable gangue such as talc, altered orthopyroxene and chlorite. Furthermore, the different types of BMS and PGM species will also play a role, to various extents, in PGM floatability, and hence recovery. In this way, the complex behaviour of composite particles can be numerically assessed. A holistic approach therefore, includes modal distribution of minerals and BMS assessment in the various concentrate cells, and is the focus of further work on these samples. In this manner, questions of floatability vs. entrainment effects during flotation can be better addressed.

Data quality remains a priority when undertaking studies involving PGM characterization, owing to the nature of the analyses, the low grades, and the very large data sets that are required to make effective comparisons and hence reach conclusions with reasonable confidence. Statistically representative data sets will determine whether significant changes in floatability can be expected in concentrate cells further down the bank, in light of their very similar PGE grades. The present study is therefore an ongoing one, with the aim to ultimately obtain a data set from which the various parameters can be modelled to provide more robust mineralogical descriptors of PGM behaviour in UG2 flotation circuits.

Acknowledgements

The authors would like to thank colleagues in the Minerals Processing Division of Mintek for performing the resampling simulations, and for flotation response information, and colleagues in the Mineralogy Division for fruitful discussion on PGMs and their flotation.

References

- @Risk, Risk analysis software package. Palisade Corporation, www.palisade.com/risk/default.asp. Accessed 31 May 2009
- BECKER, M., BROUGH, C., REID, D., SMITH, D., AND BRADSHAW, D. Geometallurgical Characterization of the Merensky Reef at Northam Platinum Mine – Comparison of Normal, Pothole and Transitional Reef Types. Ninth International Congress for Applied Mineralogy, Australasian Institute for Mining and Metallurgy, 2008. pp. 391–399.
- DOBBE, R., MOELLER, K., and SCHOUWSTRA, R. The new MLA 600F: a breakthrough FEG-SEM solution for ultra-high throughput applications in mining. FEI Company Application Note. 2008.
- FANDRICH, R., GU, Y., BURROWS, D., and MOELLER, K. Modern SEM-based mineral liberation analysis. *Int. J. Miner. Process.*, vol. 84, 2007. pp. 310–320.
- MCLAREN, C.H. and DE VILLIERS, J.P.R. The platinum-group chemistry and mineralogy of the UG-2 chromitite layer of the Bushveld Complex. *Econ. Geol.*, vol. 77, 1982. pp. 1348–1366.
- MERKLE, R.K.W. Mineralogical observations and the limits of reliability. *School on Mineralogy applied to metallurgy*. SAIMM, 27–28 July 2005.
- NEL, E., VALENTA, M., and NAUDE, N. Influence of open circuit regrind milling on UG-2 ore composition and mineralogy at Impala's UG-2 concentrator. *Minerals Engineering*, vol. 18, 2005. pp. 785–790.
- O'CONNOR, C.T. Contributions to an improved understanding of the flotation process. D.Eng thesis, University of Stellenbosch. 2005.
- PENBERTHY, C.J., OOSTHUYZEN, E.J., and MERKLE, R.K.W. The recovery of platinum-group elements from the UG-2 chromitite, Bushveld Complex—a mineralogical perspective. *Mineralogy and Petrology*, 68, 2000. pp. 213–222.
- PENBERTHY, C.J. The effect of mineralogical variation in the UG2 chromitite on recovery of platinum-group elements. PhD thesis, University of Pretoria, 2001. 410 p.
- Petruk, W. Applied Mineralogy in the Mining Industry. Elsevier, Amsterdam, 2000. 268 p.
- Resampling (Statistics) [http://en.wikipedia.org/wiki/Resampling_\(statistics\)](http://en.wikipedia.org/wiki/Resampling_(statistics)). Accessed 24 May 2009.
- SHACKLETON, N.J., MALYSIAK, V., and O'CONNOR, C.T. Surface characteristics and flotation behaviour of platinum and palladium tellurides. *Minerals Engineering*, vol. 20, 2007a. pp. 1232–1245.
- SHACKLETON, N.J., MALYSIAK, V., and O'CONNOR, C.T. Surface characteristics and flotation behaviour of platinum and palladium arsenides. *Int. J. Miner. Process.*, vol. 85, 2007b. pp. 25–40.
- SHAMAILA, S. and O'CONNOR, C.T. The role of synthetic minerals in determining the relative flotation behaviour of Platreef PGE tellurides and arsenides. *Minerals Engineering*, vol. 21, 2008. pp. 899–904.
- SUTHERLAND, D. Estimation of mineral grain size using automated mineralogy. *Minerals Engineering*, vol. 20, 2007. 452–460.
- VERMAAK, M.K.G., PISTORIUS, P.C., and VENTER, J.A. Fundamental electrochemical and Raman spectroscopic investigations of the flotation behaviour of PtAs₂. *Minerals Engineering*, vol. 20, 2007. pp. 1153–1158.
- XIAO, Z. and LAPLANTE, A.R. Characterising and recovering the platinum group minerals—a review. *Minerals Engineering*, vol. 17, 2004. pp. 961–979. ◆